phys. stat. sol. 26, 277 (1968)

Subject classification: 14.4.2; 4; 20

Battelle Institute, Geneva

Optical Study on the Ferroelectric Orthorhombic Phase of Fe–I-Boracite

By

J. Kobayashi[1]), H. Schmid, and E. Ascher

The ferro-electricity of the Fe–I-boracite is confirmed by the direct observation of domain-switching. By using this phenomenon, the birefringence in the three principal sections of the indicatrix is measured as a function of temperature. The abrupt and large change of the electrostrictive nature along the ferroelectric axis at the ferro-electric transformation is demonstrated.

Durch direkte Beobachtung von Domänenumklappungen konnte in Fe–I-Boracit Ferroelektrizität nachgewiesen werden. Unter Zuhilfenahme der Umklappung wurde die Doppelbrechung in den drei Indikatrixhauptschnitten in Abhängigkeit von der Temperatur gemessen. Es wird gezeigt, daß bei der ferroelektrischen Umwandlung längs der ferroelektrischen Achse eine plötzliche und starke Änderung der Elektrostriktion stattfindet.

1. Introduction

Some of the synthetic boracites having the chemical formula $Me_3B_7O_{13}X$, with Me = divalent metal and X = halogen, have been found to be ferroelectric; up to now, this is the case for the Mg–Cl- [1], Ni–Cl- [2], Ni–Br- [3], and Ni–I- [4] boracites. Ferro-electricity of the mineral boracite and the synthetic boracites has been questionable for a long time. It therefore appears worthwhile to demonstrate the ferro-electric behavior in some boracites unequivocally. This paper reports that the domain reversal can be discerned by optical means in the Fe–I-boracite; further, by making use of the domain reversal phenomenon, the birefringence of the three principal sections of the indicatrix is deducible from one and the same crystal orientation.

The Fe–I-boracite is isostructural with the mineral boracite $Mg_3B_7O_{13}Cl$. The structure of the high- and low-temperature form, T_d^5 and C_{2v}^5 respectively, of the latter had been worked out by Ito et al. [5]. In what follows, we use the same reference axes as those adopted in their paper. The transformation matrix from cubic to orthorhombic axes is $\frac{1}{2}, \frac{1}{2}, 0 \Big/ \frac{\bar{1}}{2}, \frac{\bar{1}}{2}, 0 \Big/ 0, 0, 1$. We designate the cubic axes as (x, y, z) and the orthorhombic axes as (X, Y, Z), the Z-axis being, of course, the unique axis in the orthorhombic phase.

2. Domain Reversal

The crystal of Fe–I-boracite was prepared by the gas-phase transportation method [6], about $2 \times 2 \times 2$ mm³ in size, and of reddish brown colour at room temperature. The transition point between high- (T_d^5) and low-temperature form (C_{2v}^5), had already been measured to be 72 °C by one of the authors [6].

---

[1]) On leave of absence from Waseda University, Tokyo.

The crystal was ground and finally polished by diamond paste on the natural (100) and (001) faces[2]); it thus became a thin (100) plate, which was transparent and almost colorless. The distances between the (100) planes and between the (001) planes were 0.211 mm and 0.396 mm, respectively. Electrodes were applied to the (001) planes by means of silver paste, and connected to a voltage source. We subjected this platelet crystal, which was accommodated in a hot-stage, to polarizing microscope observation, where the light was incident upon the (100) plane.

The crystal was at first observed as splitting into a number of twinning parts, which phenomenon was probably caused by the stresses externally applied during the grinding process. But it proved possible to reduce the numerous twinning individuals to almost a single one by the application of an electric field of about 5 kV/cm at 60 °C.

If the polarity of the external electric fields is changed so as to reverse the polarization, the interference colour of the crystal at the diagonal position changes accordingly, for instance from dark blue to yellowish orange. Examination by means of a calcite compensator showed that the Z-axis was always the optic fast axis irrespective of the polarity of the fields. Therefore it can be concluded that the refractive index of the wave oscillating along the Z-axis is the minimum and the refractive indices along the X or Y axes must be n_γ or n_β, in accord with [7]. In other words, the switching of the domains of the Fe–I boracite manifests itself as the alternation of the principal axis $n_\gamma \rightleftharpoons n_\beta$, and n_α remains unchanged. However, it has not yet been determined which axis, of the X and Y axes, corresponds to n_γ. Thus we were able to discern the switching of antiparallel domains, because of the change of interference colour. This is the salient feature of the present experiment. The relationship between the direction of applied fields and the orientation of the indicatrix is summarized in Fig. 1.

Thanks to this particular property of the indicatrix we could clearly observe the domain reversal under the appropriate electric fields. Some aspects are depicted in Fig. 2. The domain switching starts from nuclei at the electrodes, followed by forward growth of antiparallel domains (spikes) (Fig. 2a). As soon as each spike reaches the opposite crystal side, both walls of the spike begin to move sideways. Fig. 2d and 2e shows photomicrographs, taken by monochromatic light, of the sidewise motion of the walls of an antiparallel domain having weak interference colour (dark blue). As schematically shown in Fig. 2b and 2c, the domain boundary makes an angle of approximately 45° with the crystal face; it looks very diffuse because of the presence of an interference band.

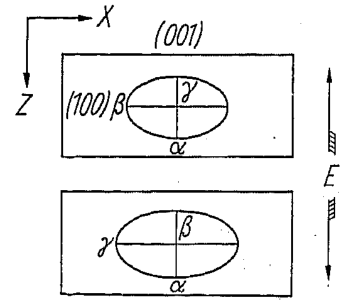

Fig. 1. Relationship between the direction of applied electric fields and the orientation of the indicatrix. The large arrow shows the direction of the electric field

---

[2]) Unless otherwise indicated in the text, the indices refer to the orthorhombic phase.

Fig. 2. Domain reversal in a (100) platelet of Fe-I-boracite. a) Nucleation of the antiparallel domains. b) Sidewise motion of 180° domain walls. The circle shows the microscopic view corresponding to Fig. 2d) and e). c) Side view of the specimen. d)–f) Photomicrographs of the 180° domains, showing the successive procession of the domain boundary and an interference band

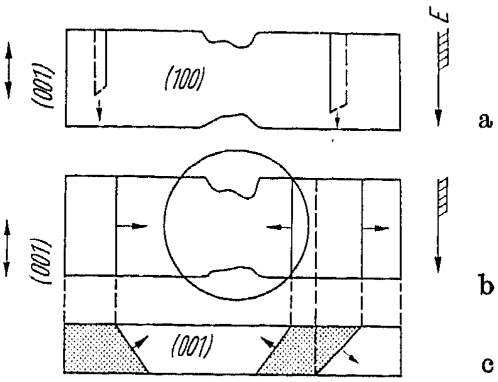

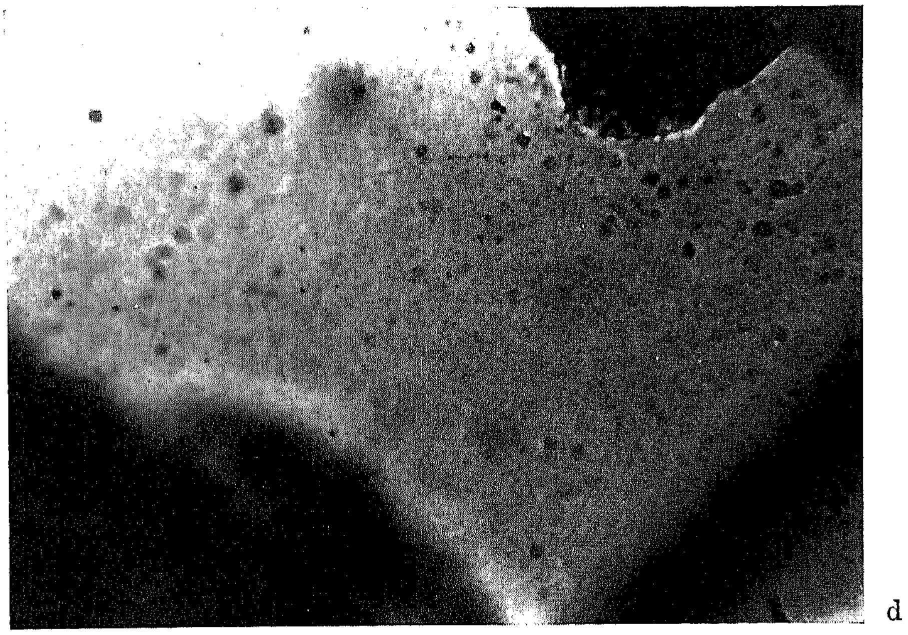

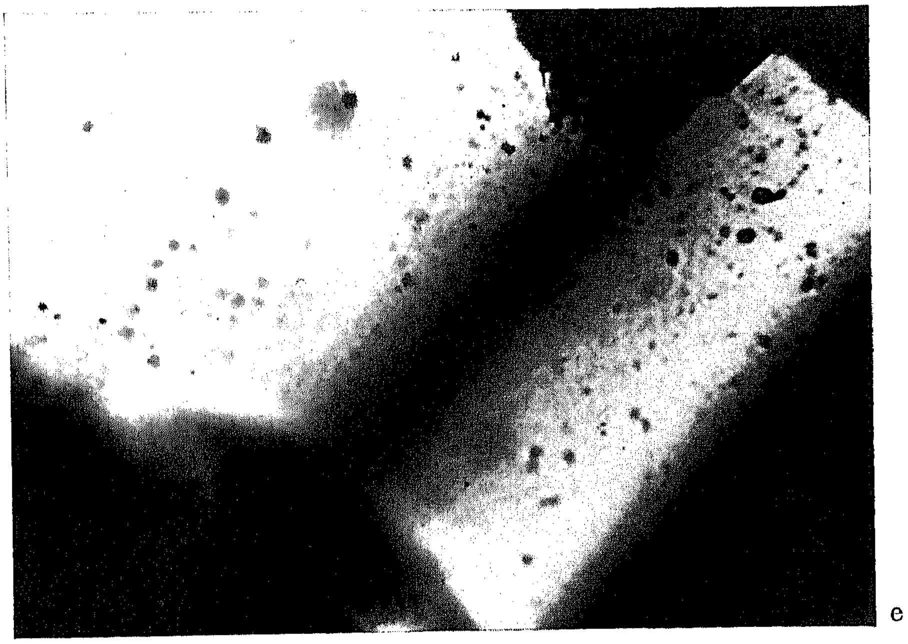

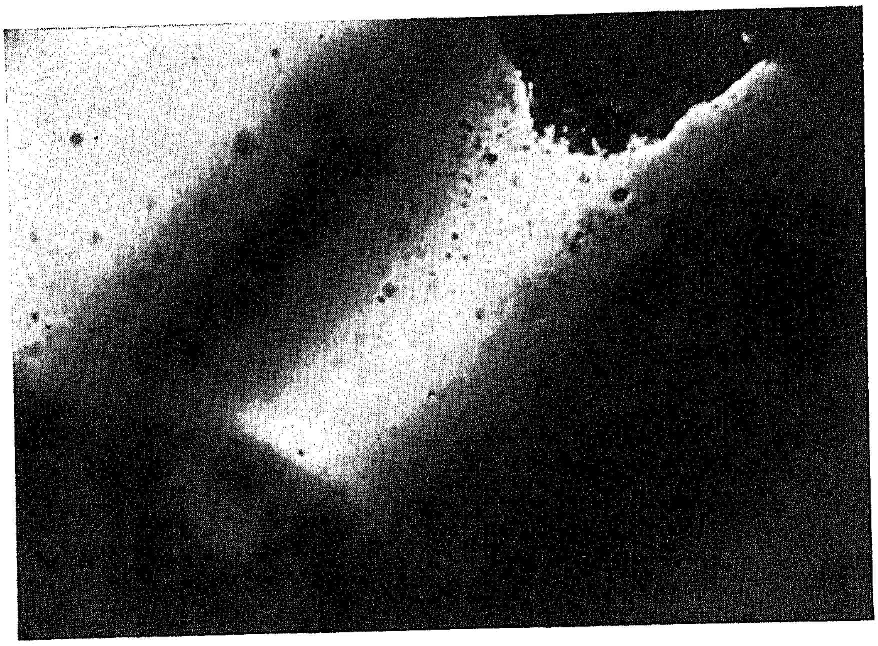

Fig. 2 f

On comparison with the switching mechanism of $BaTiO_3$ [8], there are two conspicuous features of the Fe–I-boracite, i.e. its number of nucleating domains is much smaller than that of $BaTiO_3$, and the width of each of its forward domains is very large. The velocity of the sidewise wall-motion will depend largely on the imperfections contained in the specimen.

3. Optical Anisotropy

As Fig. 1 shows, both $\Delta n_{\alpha\gamma}$ and $\Delta n_{\alpha\beta}$ can be measured by changing the polarity of the applied fields. We confirmed by the Weissenberg method that the n_β or n_γ axes exactly coincide with the crystallographic X or Y axes. This change of crystal orientation, owing to polarization reversal, can be regarded as a 180°-rotation around the orthorhombic $\langle 110 \rangle$ axis.

The temperature dependence of $\Delta n_{\alpha\gamma}$ and $\Delta n_{\alpha\beta}$ is shown in Fig. 3, the wavelength used being 5.460 Å. $n_{\gamma\beta}$, which was derived as the difference between $\Delta n_{\alpha\beta}$ and $\Delta n_{\alpha\gamma}$, is also indicated in the same figure. It is expected that the tem-

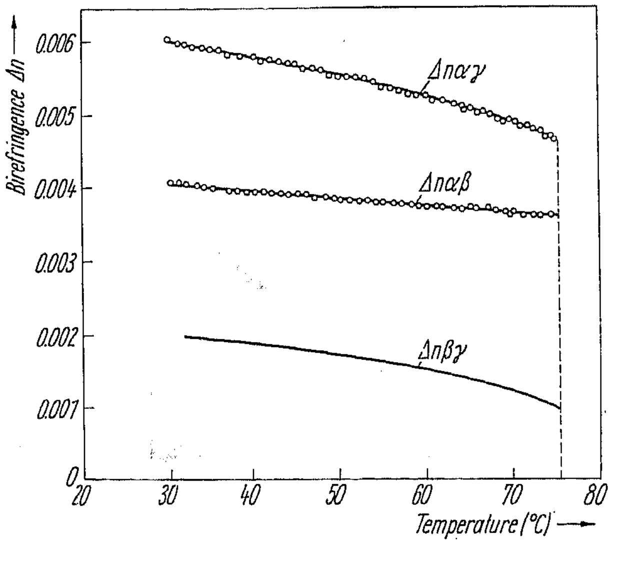

Fig. 3. Temperature dependence of the birefringence $\Delta n_{\alpha\gamma}$, $\Delta n_{\alpha\beta}$, and $\Delta n_{\beta\gamma}$ of the Fe-I-boracite

perature change of $\Delta n_{\beta\gamma}$ will be similar to that of the spontaneous polarization. The ferro-electric transition is of first order and accompanied by a temperature hysteresis of about 0.4 °C.

4. Discussion

The high-temperature form of the Fe–I-boracite, $\mathrm{T_d}$ class, has the torsional piezo-electric coefficients d_{14}, d_{25}, and d_{36}, which are all identical in sign and magnitude. Therefore, the application of an electric field E_z yields a pure shear x_y, and, accordingly, the indicatrix deforms from the sphere of radius n_0 to a triaxial ellipsoid, as schematically depicted in Fig. 4. The ferro-electric modification, $\mathrm{C_{2v}}$ class, can then be conceived as a state where the symmetry is lowered owing to the occurrence of the spontaneous polarization P_z. Consequently, it is readily suspected that antipolar domains are related by a 180°-rotation around the x-axis, as is shown in Fig. 4. As stated above, we confirmed this assumption by optical and X-ray methods.

It can be easily shown that the principal axes of the deformed indicatrix in the para-electric $\mathrm{T_d}$ phase coincide with the X, Y, Z directions. Therefore, the matrix of the electro-optic coefficients, transformed so as to be valid for these axes, and putting $2\,r_{13}^{\mathrm{p}}$ for r_{41} ($\mathrm{T_d}$), takes the following form:

$$\begin{pmatrix} 0 & 0 & r_{13}^{\mathrm{p}} \\ 0 & 0 & -r_{13}^{\mathrm{p}} \\ 0 & 0 & 0 \\ 0 & -2\,r_{13}^{\mathrm{p}} & 0 \\ 2\,r_{13}^{\mathrm{p}} & 0 & 0 \\ 0 & 0 & 0 \end{pmatrix} .$$

Then the equation of the indicatrix under the applied field E_Z is given by

$$(a_0 + r_{13}^{\mathrm{p}} E_Z)\,X^2 + (a_0 - r_{13}^{\mathrm{p}} E_Z)\,Y^2 + a_0\,Z^2 = 1\,, \tag{1}$$

where $a_0 = 1/n_0^2$ represents the relative dielectric impermeability. The refractive indices along the three axes are derived as

$$n_X^{\mathrm{p}} = n_0 - \frac{1}{2}\,n_0^3\,r_{13}^{\mathrm{p}}\,E_Z\,, \qquad n_Y^{\mathrm{p}} = n_0 + \frac{1}{2}\,n_0^3\,r_{13}^{\mathrm{p}}\,E_Z\,, \qquad n_Z^{\mathrm{p}} = n_0\,. \tag{2}$$

Thus under the E_Z field, the refractive index along the Z-axis remains unchanged (n_0), whereas those along the X and Y axes change symmetrically with respect to n_0.

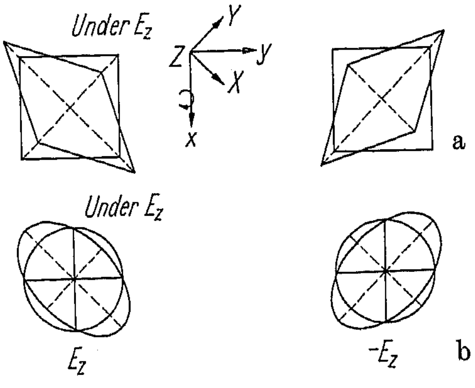

Fig. 4. Change of the spontaneous lattice strain and the indicatrix of $\mathrm{T_d}$ class owing to the applied electric field E_Z. a) lattice strain, b) indicatrix. The ring arrow shows the 180°-rotation around the x-axis

In the ferro-electric C_{2v} phase, the electro-optic coefficients are given by the following matrix:

$$\begin{pmatrix} 0 & 0 & r^{\mathrm{f}}_{13} \\ 0 & 0 & r^{\mathrm{f}}_{23} \\ 0 & 0 & r^{\mathrm{f}}_{33} \\ 0 & r^{\mathrm{f}}_{42} & 0 \\ r^{\mathrm{f}}_{51} & 0 & 0 \\ 0 & 0 & 0 \end{pmatrix}.$$

Therefore the equation of the indicatrix takes the form

$$(a_0 + r^{\mathrm{f}}_{13} E_{\mathrm{s}}) X^2 + (a_0 + r^{\mathrm{f}}_{23} E_{\mathrm{s}}) Y^2 + (a_0 + r^{\mathrm{f}}_{33} E_{\mathrm{s}}) Z^2 = 1 ,$$

where E_{s} designates the spontaneous electric field anlog the Z-axis. The refractive indices of each axis are derived as

$$n^{\mathrm{f}}_X = n_0 - \frac{1}{2} r^{\mathrm{f}}_{13} n_0^3 E_{\mathrm{s}} , \quad n^{\mathrm{f}}_Y = n_0 - \frac{1}{2} r^{\mathrm{f}}_{23} n_0^3 E_{\mathrm{s}} , \quad n^{\mathrm{f}}_Z = n_0 - \frac{1}{2} r^{\mathrm{f}}_{33} n_0^3 E_{\mathrm{s}} . \tag{3}$$

Each coefficient in the ferro-electric state can be expressed as the sum of the corresponding coefficient in the para-electric phase and the term proportional to the spontaneous electric field E_{s},

$$r^{\mathrm{f}}_{13} = r^{\mathrm{p}}_{13} + Q_1 E_{\mathrm{s}} , \quad r^{\mathrm{f}}_{23} = - r^{\mathrm{p}}_{13} + Q_2 E_{\mathrm{s}} , \quad r^{\mathrm{f}}_{33} = Q_3 E_{\mathrm{s}} , \tag{4}$$

where Q_1, Q_2, Q_3 are the electrostrictive coefficients. Then (3) can be expressed in the following form:

$$n^{\mathrm{f}}_X = n^{\mathrm{p}}_X - \frac{1}{2} Q_1 n_0^3 E_{\mathrm{s}}^2 , \quad n^{\mathrm{f}}_Y = n^{\mathrm{p}}_Y - \frac{1}{2} Q_2 n_0^3 E_{\mathrm{s}}^2 , \quad n^{\mathrm{f}}_Z = n_0 - \frac{1}{2} Q_3 n_0^3 E_{\mathrm{s}}^2 . \tag{5}$$

According to the present optical study, n^{f}_Z is the smallest of the three indices. It can therefore be concluded that Q_3 is much larger than $r^{\mathrm{p}}_{13}/E_{\mathrm{s}} + Q_1$, otherwise n^{f}_Z would lie between n^{f}_X and n^{f}_Y at the temperature region immediately below the Curie point. Electrostrictive coefficients Q_1 and Q_2 are small non-linear correction terms along the directions perpendicular to the ferro-electric axis. It will consequently be correct to regard both coefficients as nearly equal in magnitude and negligible in comparison with r^{p}_{12}/E. On the basis of this plausible assumption, the change of refractive indices can be derived from the natural refractive index n_0; for instance, $\delta n^{\mathrm{f}}_Y = \frac{1}{2} n_0^3 r^{\mathrm{p}}_{13} E_{\mathrm{s}} = \frac{1}{2} \delta n_{\gamma\beta}$. Fig. 5 represents

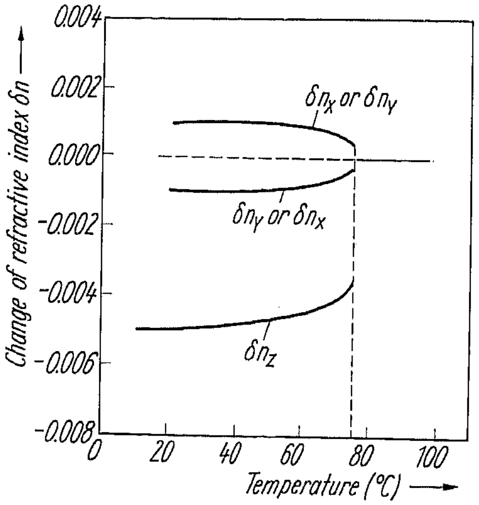

Fig. 5. Change of the refractive indices of the Fe-I-boracite in the ferro-electric state. Solid curves are derived from the observed birefringence values. The dashed line indicates the change of n^{p}_Z under the electric field

these quantities as a function of temperature, where the temperature change of n_0 is ignored, this change probably being small. The dashed line corresponds to n_Z^p under an applied electric field.

From Fig. 5 we know that n_Z is greatly decreased at the onset of the ferro-electric state, while n_X and n_Y keep essentially the slope of the para-electric state. It is of interest to note that, although the behavior of n_X and n_Y is very similar to that in KH_2PO_4 [9], the essential optical nature resembles that of $BaTiO_3$ [10]. The abrupt change of the electrostrictive nature along the ferro-electric axis at the transition must be important in the transition mechanism of Fe–I-boracite.

Ito et al. [5] reported that the orthorhombic lattice of the mineral boracite could be described as cubic so far as the dimensions are concerned. This will also be the case for the Fe-I-boracite in a rough approximation. However, knowledge of the small lattice distortions in the ferro-electric phase and of its relation to the optical anisotropy is imperative for further understanding of ferro-electricity in the boracite group. X-ray work on this line is in progress.

Acknowledgement

We are grateful to the Battelle Institute for supporting this work.

References

[1] Y. Le Corre, J. Phys. Radium **18**, 629 (1957).
[2] E. Ascher, H. Schmid, and D. Tar, Solid State Commun. **2**, 45 (1964).
[3] H. Schmid, to be published.
[4] E. Ascher, H. Rieder, H. Schmid, and H. Stössel, J. appl. Phys. **37**, 1404 (1966).
[5] T. Ito, N. Morimoto, and R. Sadanaga, Acta cryst. **4**, 310 (1951).
[6] H. Schmid, J. Phys. Chem. Solids **26**, 973 (1965).
[7] H. Schmid and J. M. Trooster, Solid State Commun. **5**, 31 (1967).
[8] For instance, J. Kobayashi, phys. stat. sol. **21**, 151 (1967).
[9] B. Zwicker and P. Scherrer, Helv. phys. Acta **17**, 346 (1944).
[10] R. Hofman, F. Gaydou, and H. Gränicher, Ferroelectric Crystals, Ed. F. Jona and G. Shirane, Pergamon Press 1962 (p. 121).

(Received December 13, 1967)